Location-Based Channel Estimation and Pilot Assignment for Massive MIMO Systems

Zhaocheng Wang*, Chen Qian*, Linglong Dai*, Jinhui Chen+, Chen Sun+, Sheng Chen†,‡
*Tsinghua National Laboratory for Information Science and Technology (TNList),
Dept. of Electronic Engineering, Tsinghua University, Beijing 100084, P. R. China.
+SONY China Research Laboratory, Beijing 100190, P. R. China.
†Electronics and Computer Science, University of Southampton, Southampton SO17 1BJ, U.K.
‡Faculty of Engineering, King Abdulaziz University, Jeddah 21589, Saudi Arabia

***Abstract*—In this paper, a location-based channel estimation algorithm is proposed for massive multi-input multi-output (MIMO) systems. By utilizing the property of the steering vector, a fast Fourier transform (FFT)-based post-processing is introduced after the conventional pilot-aided channel estimation. Under the condition that different users with the same pilot sequence have non-overlapping angle-of-arrivals (AOAs), the proposed channel estimation algorithm is capable of distinguishing these users effectively. To cooperate with the location-based channel estimation, a pilot assignment algorithm is also proposed to ensure that the users in different cells using the same pilot sequence have different AOAs at base station. The simulation results demonstrate that the proposed scheme can reduce the inter-cell interference caused by the reuse of the pilot sequence and thus improves the overall system performance significantly.**

***Index Terms*—Massive MIMO, pilot contamination, inter-cell interference, location-based channel estimation, pilot assignment**

I. Introduction

Massive multi-input multi-output (MIMO) or large-scale MIMO has been attracting lots of attentions and is regarded as a promising technology for the next generation communication systems. As reported in [1], [2], by using large number of antennas at base station (BS) to serve multiple users at the same time/frequency resource, massive MIMO can significantly improve the system performance. With the assumption of asymptotic orthogonality of the channel propagation vector, theoretical analysis [3] shows that compared with the conventional MIMO system, by using simple linear signal processing algorithm, the spectral efficiency as well as the energy efficiency of the massive MIMO are both greatly improved.

As demonstrated by Marzetta [4], the inter-cell interference (ICI) caused by the reuse of the same pilot group among cells becomes a limited factor for massive MIMO. Since the number of orthogonal pilot sequences is limited by the length of the coherence interval, it is difficult to assign orthogonal pilots to all users in different cells. Thus non-orthogonal pilot sequences have to be applied, and the channel estimation at each BS will be contaminated by the pilots sent from other cells. This pilot contamination effect limits the performance of massive MIMO systems, since unlike noise and intra-cell interference, this ICI will not vanish even when the number of antennas at BS goes to infinity. The current solutions to pilot contamination can be divided into two categories.

The first category is based on the pilot design and pilot allocation. For example, in [5], a pilot design method for massive MIMO is proposed. By maximizing the signal-to-interference ratio (SIR), a design criterion is introduced. This kind of solutions cannot completely eliminate the ICI caused by the pilot contamination, since the reuse of the same pilot group is still required. The second category includes "smart" signal processing algorithms. As pointed out in [6], the pilot contamination can be regarded as a shortage of linear processing algorithms and a sub-space based blind channel estimation algorithm is proposed to reduce the ICI. In [7], a Bayesian estimator is applied to massive MIMO which requires the second-order statics of the channel coefficients. To further mitigate the ICI, a pilot assignment is also proposed which requires the cooperation between BSs. In [8], the pilot contamination precoding is proposed and the large-scale fading coefficients of users in different cells are utilized to eliminate the ICI. Although the non-linear signal processing algorithms can significantly reduce the ICI caused by pilot contamination, their complexity is usually high and some *a priori* information, such as channel covariance matrix, is required at BS.

In this paper, a location-based channel estimation algorithm is proposed. After the conventional pilot-aided channel estimation, a fast Fourier transform (FFT)-based post-processing is introduced. The proposed algorithm can efficiently distinguish the users with different angle of arrivals (AOAs). The ICI caused by pilot contamination is reduced if the users in different cells with the same pilot have non-overlapping AOAs. To cooperate with the channel estimation algorithm, a location-based pilot assignment is also proposed to ensure the condition of non-overlapping AOAs. Our solution differs from [7] in that, instead of minimizing the mean square error of the channel estimation, our algorithm aims at separating different users by exploiting the degrees of freedom in spatial domain and the knowledge of the channel covariance matrix is not required. Moreover, coordination between BSs is not necessary, which means that the proposed scheme is more suitable for practical implementation. Simulation results show that our scheme can reduce the ICI significantly and improve the overall system performance with only slightly increase in complexity.

II. System Model

Consider a homogeneous multi-cell multi-user MIMO system with L hexagonal cells. In each cell, K users with single antenna are served at the same time/frequency resource. The BS within each cell is equipped with M antennas with $M \gg K$. To prevent the loss of spectral efficiency caused by the large overhead of downlink pilots, time division duplex (TDD) is applied. When analyzing the channel estimation algorithm, we assume $K = 1$ to simplify the analysis. This assumption is equivalent to assume that the same K orthogonal pilots are used in every cell.

The transmission is divided into three stages. In the first stage, the users from all the cells transmit the pilot signals to their corresponding BSs. The pilot sequences used by the users in the same cell are orthogonal and the same pilot group is re-used by all the cells. The length of the pilot sequences is limited by the channel coherence time τ. Denote $\boldsymbol{\phi} = [\phi_1 \ \phi_2 \cdots \phi_\tau]$ as the pilot sequence with length τ, where $\boldsymbol{\phi}\boldsymbol{\phi}^{\mathrm{H}} = 1$. In the first stage, the received signal of the BS in the l-th cell can be written as

$$\boldsymbol{Y}_l = \sum_{j=1}^{L} \boldsymbol{h}_{l,j}\boldsymbol{\phi} + \boldsymbol{N}_l, \tag{1}$$

where $\boldsymbol{Y}_l \in \mathbb{C}^{M\times\tau}$ and $\boldsymbol{N}_l \in \mathbb{C}^{M\times\tau}$ denote the received signal matrix and the additive white Gaussian noise (AWGN) matrix, respectively, while $\boldsymbol{h}_{l,j} = [h_{l,j,1} \ h_{l,j,2} \cdots h_{l,j,M}]^{\mathrm{T}}$ is the channel coefficient vector with $h_{l,j,i}$ denoting the channel coefficient between the user in the j-th cell and the i-th antenna of the BS in the l-th cell. At the BS, the orthogonality of the pilot sequences is used for channel estimation. For the user in the l-th cell, we multiply $\boldsymbol{Y}_l$ by $\boldsymbol{\phi}^{\mathrm{H}}$ to obtain

$$\widehat{\boldsymbol{h}}_{l,l} = \boldsymbol{Y}_l\boldsymbol{\phi}^{\mathrm{H}} = \boldsymbol{h}_{l,l} + \sum_{j\neq l} \boldsymbol{h}_{l,j} + \boldsymbol{\varepsilon}_l, \tag{2}$$

where $\boldsymbol{\varepsilon}_l = \boldsymbol{N}_l\boldsymbol{\phi}^{\mathrm{H}}$ is the equivalent noise vector at the channel estimate. Note that here we apply the simplest pilot-aided channel estimation since realistically the BS has no knowledge of the channel covariance matrix. Obviously, such a conventional channel estimation alone cannot cancel the ICI caused by the non-orthogonal pilot sequences between the users in different cells, which limits the system performance.

In the second stage, the users transmit data to the BSs. The received signal of the l-th BS is written as

$$\boldsymbol{y}_l = \sum_{j=1}^{L} \boldsymbol{h}_{l,j}s_j + \boldsymbol{n}_l, \tag{3}$$

where $s_j \in \mathbb{C}$ is the symbol transmitted by the user in the j-th cell with $E\{|s_j|^2\} = 1$, $\boldsymbol{y}_l \in \mathbb{C}^{M\times 1}$ is the received vector and $\boldsymbol{n}_l \in \mathbb{C}^{M\times 1}$ denotes the AWGN vector. The channel estimation $\widehat{\boldsymbol{h}}_{l,l}$ obtained in the first stage is used in detection. The detected symbol for the user in the l-th cell is given as

$$\widehat{s}_l = \boldsymbol{A}_l\boldsymbol{y}_l, \tag{4}$$

where $\boldsymbol{A}_l \in \mathbb{C}^{1\times M}$ is the detector coefficient matrix calculated based on $\widehat{\boldsymbol{h}}_{l,l}$. In this paper, we apply the zero-forcing (ZF) detection with $\boldsymbol{A}_l = \big(\widehat{\boldsymbol{h}}_{l,l}^{\mathrm{H}}\widehat{\boldsymbol{h}}_{l,l}\big)^{-1}\widehat{\boldsymbol{h}}_{l,l}^{\mathrm{H}}$.

In the third stage, the BSs transmit data to their corresponding users. The channel reciprocity of the TDD system is utilized, implying that the downlink channel matrix is the transpose of the uplink channel matrix. Let d_l be the symbol transmitted by the l-th BS to its corresponding user with $E\{|d_l|^2\} = 1$. The received signal of the user in the l-th cell is given by

$$r_l = \sum_{j=1}^{L} \boldsymbol{h}_{j,l}^{\mathrm{T}}\boldsymbol{W}_j d_j + n_l, \tag{5}$$

where $n_l \in \mathbb{C}$ denotes the channel AWGN, while $\boldsymbol{W}_j$ is the precoding matrix for the user in the j-th cell and is calculated based on the channel estimation obtained in the first stage. Considering the fact that ZF-precoding is easy to implement and it approaches the optimal performance when M tends to infinity, we apply the ZF-precoding algorithm which calculates the precoding matrix according to $\boldsymbol{W}_l = \beta\widehat{\boldsymbol{h}}_{l,l}^{*}\big(\widehat{\boldsymbol{h}}_{l,l}^{\mathrm{T}}\widehat{\boldsymbol{h}}_{l,l}^{*}\big)^{-1}$, where β is the normalization factor and $[\cdot]^*$ denotes the conjugate operation.

We adopt the following narrow-band multi-path channel model [7]

$$\boldsymbol{h}_{n,l} = \frac{1}{\sqrt{P}}\sum_{p=1}^{P} \boldsymbol{a}(\theta_{n,l,p})\beta_{n,l,p}, \tag{6}$$

where P is the number of the paths between the user in the l-th cell and the BS in the n-th cell, $\beta_{n,l,p}$ denotes the large-scale fading parameter of the p-th path, which includes the path-loss and the shadow fading, and $\theta_{n,l,p}$ is the AOA of the p-th path, while the vector $\boldsymbol{a}(\theta) \in \mathbb{C}^{M\times 1}$ is the steering vector with the AOA θ, where $\theta \in [0, \pi]$. For the uniformly-spaced linear array (ULA), the steering vector $\boldsymbol{a}(\theta)$ is given by [9]

$$\boldsymbol{a}(\theta) = \Big[1 \ e^{-\mathrm{j}2\pi\frac{D}{\lambda}\cos(\theta)} \cdots e^{-\mathrm{j}2\pi\frac{(M-1)D}{\lambda}\cos(\theta)}\Big]^{\mathrm{T}}, \tag{7}$$

where λ is the wavelength of the received signal and $D \leq \lambda/2$ is the antenna spacing at BS. Note that this narrow-band channel model can be extended to the wide-band system by utilizing orthogonal frequency division multiplexing (OFDM) technique.

We assume that the angular spread of AOA is small, and thus $\theta_{n,l,p} \in \big[\theta_{min}^{n,l}, \ \theta_{max}^{n,l}\big]$, for $1 \leq p \leq P$. As pointed out in [10], this assuption holds when the BS is much higher than the surrounded structures with few scatters around. This scenario reflects the macro cell or micro cell environments.

III. Location-based channel estimation

We now detail our proposed location-based channel estimation algorithm. Specifically, under the condition that the AOAs of different users do not overlap, a post-processing is introduced after the conventional pilot-aided channel estimation of Eq. (2). By utilizing the properties of steering vector, the interference from the users with different AOAs can be reduced.

The property of steering vector is first described. By observing the steering vector $\boldsymbol{a}(\theta)$ in Eq. (7), we can see that $\boldsymbol{a}(\theta)$ can be regarded as a single-frequency signal with the frequency $f_{\boldsymbol{a}} = \frac{D}{\lambda}\cos(\theta)$. Thus when the number of the antennas at the BS goes towards infinity, the Fourier transform of $\boldsymbol{a}(\theta)$ tends to a δ-function. The basic idea is to utilize this property to distinguish the users with different AOAs.

The N-points discrete Fourier transform (DFT) of the steering vector given in Eq. (7) is calculated by

$$X(k) = \sum_{m=0}^{M-1} a(m) e^{-\mathrm{j}\frac{2\pi}{N}km} = \frac{1-e^{-\mathrm{j}2\pi M\left(\frac{D}{\lambda}\cos(\theta)+\frac{k}{N}\right)}}{1-e^{-j2\pi\left(\frac{D}{\lambda}\cos(\theta)+\frac{k}{N}\right)}}, \quad (8)$$

for $0 \leq k \leq N-1$, where $a(m) = e^{-\mathrm{j}2\pi\frac{mD}{\lambda}\cos(\theta)}$, $m = 0, 1, \cdots, M-1$, is the m-th element of $\boldsymbol{a}(\theta)$. By using the property of $1-x^M = (1-x)(1+x+x^2+\cdots+x^{M-1})$ and letting $q_k = \frac{D}{\lambda}\cos(\theta)+\frac{k}{N}$, we can simplify (8) as

$$X(k) = \frac{(1-e^{-\mathrm{j}2\pi q_k})(\sum_{i=0}^{M-1} e^{-\mathrm{j}2\pi i q_k})}{1-e^{-\mathrm{j}2\pi q_k}} = \sum_{i=0}^{M-1} e^{-\mathrm{j}2\pi i q_k}. \quad (9)$$

Considering that each term in Eq. (9) has unit norm, the following expression holds

$$|X(k)| = \Big|\sum_{i=0}^{M-1} e^{-\mathrm{j}2\pi i q_k}\Big| \leq M,\ k = 0, \cdots, N-1. \quad (10)$$

If and only if $e^{-\mathrm{j}2\pi i q_k} = 1$ for every $0 \leq i \leq M-1$ in (10), the norm of $X(k)$ attains its maximal value M. This means that when q_k is an integer, i.e. $q_k = \frac{D}{\lambda}\cos(\theta)+\frac{k}{N} \in \mathbb{Z}$, the maximal value M is attained. Let $k_{lim} = \arg\max_{0\leq k\leq N-1}|X(k)|$, we have $k_{lim} = [\![g_N(\theta)]\!]$, where $[\![\cdot]\!]$ denotes the integer rounding operation, and the function $g_N(\theta)$ is written as

$$g_N(\theta) = \begin{cases} N - N\frac{D}{\lambda}\cos(\theta), \theta \in [0, \pi/2) \\ -N\frac{D}{\lambda}\cos(\theta), \theta \in [\pi/2, \pi], \end{cases} \quad (11)$$

If $N\frac{D}{\lambda}\cos(\theta) \notin \mathbb{Z}$, $|X(k_{lim})|$ cannot reach the maximal value M, but $|X(k_{lim})|$ is still very close to M since each term $e^{-\mathrm{j}2\pi i q_{k_{lim}}}$ in (10) is close to 1.

Denote the FFT of the estimated channel coefficient vector $\widehat{\boldsymbol{h}}_{l,l}$ as $\boldsymbol{F}_{l,l} = \left[F_{l,l}(0)\ F_{l,l}(1)\cdots F_{l,l}(N-1)\right]^{\mathrm{T}}$. Under the assumption that the AOA of the user in the l-th cell is limited in the interval $[\theta^l_{min},\ \theta^l_{max}]$, we can utilize the above-described property to force the value of $\boldsymbol{F}_{l,l}$ outside the interval $I(k^l_{min},\ k^l_{max})$ to zero, where $I(k^l_{min},\ k^l_{max})$ is defined by

$$I(k^l_{min}, k^l_{max}) = \begin{cases} [0, k^l_{max}] \cup [k^l_{min}, N], \\ \qquad 0 \leq \theta^l_{min} < \pi/2 < \theta^l_{min} \leq \pi \\ [k^l_{min},\ k^l_{max}], otherwise, \end{cases}$$

k^l_{min} and k^l_{max} are calculated as

$$\begin{cases} k^l_{min} = [\![g_N(\theta^l_{min})]\!], \\ k^l_{max} = [\![g_N(\theta^l_{max})]\!]. \end{cases} \quad (12)$$

In this way, the signals with the AOAs outside the interval $\left[\theta^l_{\mathrm{min}},\ \theta^l_{max}\right]$ are canceled out. Besides, the effect of the noise is also reduced. With this cancellation, we have

$$\widehat{F}_{l,l}(k) = \begin{cases} F_{l,l}(k), & k \in I(k^l_{min},\ k^l_{max}), \\ 0, & k \notin I(k^l_{min},\ k^l_{max}). \end{cases} \quad (13)$$

Perform the inverse FFT (IFFT) on $\widehat{\boldsymbol{F}}_{l,l} = \left[\widehat{F}_{l,l}(0)\ \ \widehat{F}_{l,l}(1)\cdots\widehat{F}_{l,l}(N-1)\right]^{\mathrm{T}}$ and denote the result as $\widehat{\boldsymbol{f}}_{l,l} = \left[\widehat{f}_{l,l}(0)\ \widehat{f}_{l,l}(1)\cdots\widehat{f}_{l,l}(N-1)\right]^{\mathrm{T}}$. The estimation of the channel coefficient vector is obtained as

$$\bar{\boldsymbol{h}}_{l,l} = \left[\widehat{f}_{l,l}(0)\ \widehat{f}_{l,l}(1)\cdots\widehat{f}_{l,l}(M-1)\right]^{\mathrm{T}}. \quad (14)$$

It should be noted that (13) is actually the operation that places a rectangle window on $\boldsymbol{F}_{l,l}$ to perform a filtering operation in the spatial domain. Selection of different windows can lead to different performance of channel estimation.

IV. Location-based pilot assignment

As mentioned in the previous section, the proposed location-based estimation method requires the condition of non-overlapping AOAs of different users. To satisfy this assumption, a location-based pilot assignment is introduced. The main idea is to make sure that the users in different cells with the same pilot sequence have different AOAs at the BS.

To simplify the analysis, a hexagonal cell is divided into S sectors. Denote Θ^s_{max} and Θ^s_{min} as the maximal and minimal AOAs of the users in the s-th sector, respectively. We assume that $\Delta\Theta^s = \Theta^s_{max} - \Theta^s_{min} = \Delta\Theta = \frac{2\pi}{S}$ is the same for all the sectors. Each sector is assigned with one pilot sequence and all the users within one sector use the same pilot. The pilot sequences assigned to different sectors are orthogonal. To serve multiple users at the same time/frequency resource, the BS selects one user from each sector, according to the assigned pilots. For multi-cell pilot assignment, we propose that two principles should be considered.

The first one is that the sectors in different cells with the same pilot sequence should have different AOAs at BSs. This principle ensures that the users with the same pilot have non-overlapping AOAs and thus the performance of the location-based channel estimation can be improved significantly.

The second principle is that if it is difficult to ensure the non-overlapping AOAs for the users with the same pilot, the distance between the interference sector and the BS of the cell considered should be sufficiently large. Thus if the non-overlapping condition cannot be satisfied, the path loss should be utilized to reduce the potential ICI sufficiently.

To apply these two principles, we assume that there is a representative user located in the center of each sector. Let $\theta_{n,s,l}$ be the AOA of the representative user in the s-th sector of the l-th cell at the n-th cell's BS, and $d_{n,s,l}$ be the distance between this representative user and the n-th cell's BS. To investigate the ICI of the interference cells to the n-th cell, the following metric is proposed for the pilot assignment

$$R_{n,s,l} = \frac{|\mathbf{t}^{\mathrm{T}}(\theta_{n,s,n})\mathbf{t}(\theta_{n,s,l})|}{d^{\gamma}_{n,s,l}}, \quad (15)$$

where $\mathbf{t}(\theta) = [\cos(\theta)\ \ \sin(\theta)]^{\mathrm{T}}$ is the directional vector with unit length and γ is the path-loss exponent. Since $R_{n,s,l}$ defined in (15) measures not only the correlation between the two AOAs but also the distance of the interference user, it is a good metric for measuring the ICI between the s-th sectors of the l-th cell and the n-th cell. Smaller $R_{n,s,l}$ indicates smaller ICI.

By applying the metric $R_{n,s,l}$ defined in (15), the optimal pilot assignment can be obtained by exhaustively searching all the possible patterns to find the solution with the minimal value of $\sum_n \sum_s \sum_l R_{n,s,l}$. However, the exponential complexity of exhaustive search is too high in practice, especially when the number of cells is large. Fortunately, the interference caused by the adjacent sectors is the severest and owing to the path-loss, the interference of the far-away sectors is much smaller. We assume that there is one cell that has been assigned with pilots and we consider the sectors in its adjacent cells. Under this scenario, we provide a two-step simplified method.

In the first step, the sectors in the adjacent cells are assigned by non-exhaustive search. Specifically, for a sector that has been assigned with pilot, the adjacent sectors in its nearest cell are checked by calculating their corresponding metrics $R_{n,s,l}$, and the sector with the smallest $R_{n,s,l}$ is selected to assign with the same pilot sequence. After all the possible sectors are checked and assigned, there will be still some blank sectors located on the edges of the network that need to be assigned.

In the second step, these remaining sectors are assigned with pilots by exhaustive search and the assignment is based on the smallest $\sum_s R_{n,s,l}$. The summations over n and l have been removed because in the first step, the sectors in the nearest cells are assigned and the remaining sectors will not affect their interference cells. Normally, the number of the blank sectors left in each cell is small and the complexity of the second-step exhaustive search based assignment is reduced significantly.

It should be noted that the aforementioned pilot assignment is static and needs to be performed only once. For users with high mobility, a dynamic pilot assignment is required to ensure the non-overlapping assumption, which is our future work.

V. Numerical Results

The simulation results are used to demonstrate the efficiency of the proposed scheme. A multi-cell multi-user MIMO scenario with $L = 7$ is considered and each cell is divided into $S = 12$ sectors, which means that at most 12 users can be served at the same time/frequency resource. The users in the center cell are the target users and the surrounded cells are regarded as the interference cells. Some basic simulation parameters are listed in table I.

TABLE I
BASIC SIMULATION PARAMETERS

Cell radius	500m
Path loss exponent	3.5
Variance of shadow fading	8 dB
Carrier frequency	2 GHz
Antenna spacing D	λ/2
Number of paths per user P	50
Angle spread	10 degrees

For the center cell, which is denoted by cell 0, the distance between all the users and the BS is larger than 400 m. As a result, the ICI is server if the conventional channel estimation (2) is applied. For the interference cells, which are denoted by cell 1 to 6, the users are randomly generated and each sector has one user. For the location-based channel estimation, the size of FFT is fixed to $N = 8192$. We also assume that the system works in a noise-free environment in order to focus on the effects of ICI. The two-step pilot assignment method proposed in Section IV is applied. The angle spread δ_θ is 10 degrees and two distributions of angle spread are considered. The first one is the uniform distribution in which the AOAs are uniformly distributed in $\left[\theta_c - \delta_\theta/2,\ \theta_c + \delta_\theta/2\right]$, where θ_c is the AOA with line of sight. The second one is Gaussian distribution with mean θ_c and variance $(\delta_\theta/2)^2$.

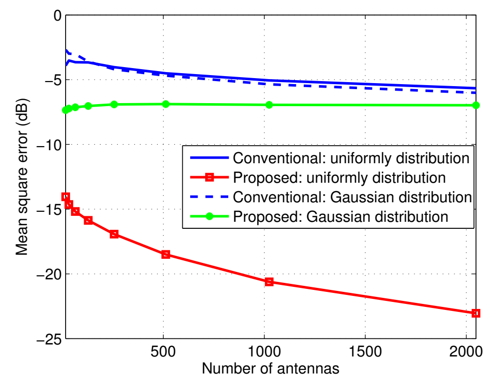

Fig. 1. MSEs of the different channel estimation methods.

Let $\widehat{\boldsymbol{h}}$ and $\boldsymbol{h}$ be the estimated and real channel coefficient vectors, respectively. Then the mean square error (MSE) of channel estimation is defined as

$$\mathrm{MSE} = 10\log_{10}\left(\frac{E\{\|\widehat{\boldsymbol{h}} - \boldsymbol{h}\|^2\}}{E\{\|\boldsymbol{h}\|^2\}}\right)\ [\mathrm{dB}]. \tag{16}$$

The MSEs of the location-based channel estimation and the conventional channel estimation shown in Fig. 1 clearly demonstrate the superior performance of the proposed scheme over the conventional one. In particular, for the case of uniformly distributed angle spread, the location-based channel estimation improves the MSE significantly. With $M \simeq 100$, its MSE is about -15 dB, achieving more than 10 dB gain over its conventional counterpart. Furthermore, as the number of antennas M increases, its MSE reduces significantly. However, it seems that the proposed method is not as efficient for the Gaussian distributed angle spread, and its MSE is not reduced when M increases. This is caused by the fact that the AOAs are not bounded in an interval and some useful paths are filtered out. Because most of the interference is canceled in our proposed channel estimation, this loss of MSE performance under the Gaussian distributed angle spread will not affect the overall system performance significantly, as will be shown later.

The per user spectral efficiency of the uplink data transmission is investigated. To simplify analysis, we still assume that there is only one user in each cell. The uplink spectral efficiency of the user in sector s is written as

$$C_s^u = \log_2\left(1 + \mathrm{SIR}_s^u\right), \tag{17}$$

in which the uplink SIR of the user in sector s of the center cell, SIR_s^u, is computed by

$$\mathrm{SIR}_s^u = \frac{E\{\|\boldsymbol{A}_{s,0}\boldsymbol{h}_{0,s,0}\|^2\}}{E\{\|\boldsymbol{A}_{s,0}\sum_{i\neq 0}\boldsymbol{h}_{0,s,i}\|^2\}}, \tag{18}$$

where $\boldsymbol{A}_{s,l}$ is the detection matrix of the s-th sector in the l-th cell, and $\boldsymbol{h}_{l_1,s,l_2}$ is the channel matrix from the s-th sector of l_2-th cell to the BS in the l_1-th cell. The ZF detection is applied. Fig. 2 shows the uplink spectral efficiency results, where it can be seen that the uplink spectral efficiency of the

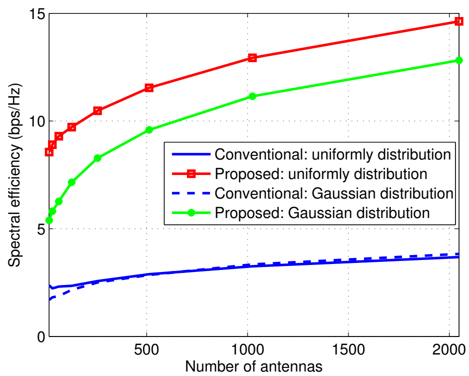

Fig. 2. Per user spectral efficiency of uplink data transmission.

proposed method is improved significantly compared with the conventional method. When $M \simeq 100$, the data rates of the proposed scheme are higher than 8 bps/Hz and 5 bps/Hz for the uniformly and Gaussian distributed angle spreads, respectively, while the spectral efficiency of the conventional method is lower than 3 bps/Hz.

For the downlink data transmission, the spectral efficiecy of the user in the s-th sector is computed as

$$C_s^d = \log_2 \left(1 + \mathrm{SIR}_s^d\right), \tag{19}$$

in which SIR_s^d is the downlink SIR of the user in sector s of cell 0 and is given by

$$\mathrm{SIR}_s^d = \frac{E\{\|\boldsymbol{h}_{0,s,0}^{\mathrm{T}} \boldsymbol{W}_{s,0}\|^2\}}{E\{\| \sum_{i\neq 0} \boldsymbol{h}_{i,s,0}^{\mathrm{T}} \boldsymbol{W}_{s,i}\|^2\}}, \tag{20}$$

where $\boldsymbol{W}_{s,l}$ is the precoding matrix for the user in the s-th sector of the l-th cell. Again the ZF precoding is applied. As expected, the results shown in Fig. 3 confirm that the downlink spectral efficiecy is also improved significantly by using the proposed scheme, and the gain is more than 4 bps/Hz compared with the conventional method when $M = 100$.

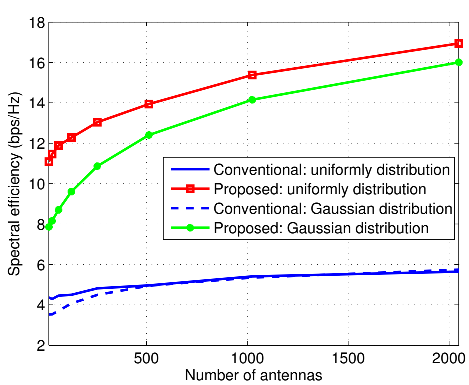

Fig. 3. Per user spectral efficiency of downlink data transmission.

Recall that the MSE of the location-based channel estimation does not reduce with the increase of M for the Gaussian distributed angle spread. However, observe from Figs. 2 and 3 that with the Gaussian distributed angle spread, the spectral efficiency increases as M increases, and the gain is significant. This is because with larger M, the resolution of different AOAs is better. Thus the users with different AOAs can be distinguished more accurately and the ICI caused by the reuse of pilots is also reduced, resulting in a better performance.

Note that compared with the conventional method, the proposed scheme still offers a low complexity since only additional FFT and IFFT operations are added. The pilot assignment can be carried out in cell planing stage, and no coordination between BSs is required during channel estimation.

VI. Conclusions

A location-based channel estimation algorithm has been proposed, which introduces an FFT-based post-processing after the conventional pilot-aided channel estimation to utilize the steering vector for mitigating the inter-cell interference. Our analysis has shown that if the users with the same pilot sequence have different AOAs at the BS, they can be distinguished using the proposed channel estimation algorithm. A location-based pilot assignment has also been proposed to ensure the condition of the non-overlapping AOAs to further improve the system performance. Simulation results have demonstrated that compared with the conventional channel estimation, our location-based scheme can improve the uplink and downlink spectral efficiency significantly with a slightly increased complexity.

Acknowledgment

This work was supported by National High Technology Research and Development Program of China (Grant No. 2014AA01A704), Beijing Natural Science Foundation (Grant No. 4142027), and Information Technology Development Division, Sony Corporation and Sony China Research Laboratory, Sony (China) Ltd.

References

[1] F. Rusek, D. Persson, B. K. Lau, E. Larsson, T. Marzetta, O. Edfors, and F. Tufvesson, "Scaling up MIMO: Opportunities and challenges with very large arrays," *IEEE Signal Processing Magazine*, vol. 30, no. 1, pp. 40–60, Jan. 2013.

[2] E. Larsson, O. Edfors, F. Tufvesson, and T. Marzetta, "Massive MIMO for next generation wireless systems," *IEEE Communications Magazine*, vol. 52, no. 2, pp. 186–195, Feb. 2014.

[3] H. Q. Ngo, E. Larsson, and T. Marzetta, "Energy and spectral efficiency of very large multiuser mimo systems," *IEEE Trans. Commun.*, vol. 61, no. 4, pp. 1436–1449, Apr. 2013.

[4] T. Marzetta, "Noncooperative cellular wireless with unlimited numbers of base station antennas," *IEEE Trans. Wireless Commun.*, vol. 9, no. 11, pp. 3590–3600, Nov. 2010.

[5] A. Hu, T. Lv, H. Gao, Y. Lu, and E. Liu, "Pilot design for large-scale multi-cell multiuser MIMO systems," in *Proc. ICC 2013* (Budapest, Hungary), June 9-13, 2013, pp. 5381–5385.

[6] R. R. Müeller, M. Vehkaperae, and L. Cottatellucci, "Blind pilot decontamination," in *Proc. 17th Int. ITG Workshop on Smart Antennas (WSA 2013)*, March 13-14, 2013, pp. 1–6.

[7] H. Yin, D. Gesbert, M. Filippou, and Y. Liu, "A coordinated approach to channel estimation in large-scale multiple-antenna systems," *IEEE J. Sel. Areas Commun.*, vol. 31, no. 2, pp. 264–273, Feb. 2013.

[8] A. Ashikhmin and T. Marzetta, "Pilot contamination precoding in multi-cell large scale antenna systems," in *Proc. 2012 IEEE Int. Symp. Information Theory Proceedings (ISIT 2012)* (Cambridge, MA), July 1-6, 2012, pp. 1137–1141.

[9] J. Wang, C. Huang, J. Zhou, and H. Kikuchi, "The impact of AOA energy distribution on the spatial fading correlation and SER performance of a circular antenna array," in *Proc. 2006 IFIP Int. Conf. Wireless and Optical Communications Networks* (Bangalore, India), April 11-13, 2006, pp. 933–937.

[10] K. Yu and B. Ottersten, "Models for MIMO propagation channels: A review," *J. Wireless Commun. Mob. Comput.*, vol. 2, no. 7, pp. 653–666, Nov. 2002.